

01 Jan 1983

Collisions Of Fast Highly Charged Ions In Gas Targets: Ionization, Recoil-Ion Production, And Charge Transfer

A. S. Schlachter

K. H. Berkner

H. F. Beyer

W. G. Graham

et. al. For a complete list of authors, see https://scholarsmine.mst.edu/phys_facwork/2545

Follow this and additional works at: https://scholarsmine.mst.edu/phys_facwork

 Part of the [Physics Commons](#)

Recommended Citation

A. S. Schlachter and K. H. Berkner and H. F. Beyer and W. G. Graham and W. Groh and R. Mann and A. Müller and R. E. Olson and R. V. Pyle and J. W. Stearns and J. A. Tanis, "Collisions Of Fast Highly Charged Ions In Gas Targets: Ionization, Recoil-Ion Production, And Charge Transfer," *Physica Scripta*, vol. 1983, no. T3, pp. 153 - 158, IOP Publishing; Royal Swedish Academy of Sciences, Jan 1983.
The definitive version is available at <https://doi.org/10.1088/0031-8949/1983/T3/029>

This Article - Journal is brought to you for free and open access by Scholars' Mine. It has been accepted for inclusion in Physics Faculty Research & Creative Works by an authorized administrator of Scholars' Mine. This work is protected by U. S. Copyright Law. Unauthorized use including reproduction for redistribution requires the permission of the copyright holder. For more information, please contact scholarsmine@mst.edu.

Collisions of Fast Highly Charged Ions in Gas Targets: Ionization, Recoil-Ion Production, and Charge Transfer

To cite this article: A S Schlachter *et al* 1983 *Phys. Scr.* **1983** 153

View the [article online](#) for updates and enhancements.

You may also like

- [Recoil-ion production cross sections and differential scattering angle dependences in 2.5-15 MeV \$F^{n+}\$ \(\$n=4, 6, 8\$ \) on Ne collisions](#)
S Kelbch, C L Cocke, S Hagmann et al.
- [Multiple ionisation effects due to recoil in atomic collisions](#)
L Vegh
- [Measurement of the mean transverse kinetic energy of recoil ions produced in energetic electron-atom collisions](#)
R K Singh, S Mondal and R Shanker

Collisions of Fast Highly Charged Ions in Gas Targets: Ionization, Recoil-Ion Production, and Charge Transfer

A. S. Schlachter,^{1†} K. H. Berkner,¹ H. F. Beyer,² W. G. Graham,³ W. Groh,⁴ R. Mann,² A. Müller,⁴ R. E. Olson,⁵ R. V. Pyle,¹ J. W. Stearns¹ and J. A. Tanis⁶

¹Lawrence Berkeley Laboratory, University of California, Berkeley, California 94720, U.S.A.; ²Gesellschaft für Schwerionenforschung, 6100 Darmstadt, Federal Republic of Germany; ³The New University of Ulster, Coleraine, Northern Ireland; ⁴Institut für Kernphysik, Strahlenzentrum, Universität Giessen, 6300 Giessen, Federal Republic of Germany; ⁵Department of Physics, University of Missouri-Rolla, Rolla, Missouri 65401, U.S.A.; ⁶Department of Physics, Western Michigan University, Kalamazoo, Michigan 49008, U.S.A.

Received August 2, 1982; accepted October 28, 1982

Abstract

Electron-capture, ionization, and recoil-ion-production cross-sections are measured and calculated for fast highly charged projectiles in hydrogen and rare-gas targets. Recoil-ion-production cross-sections are found to be large; the low energy and high charge states of the recoil ions make them useful for subsequent collision studies.

1. Introduction

Collisions of fast highly charged projectiles with gas targets are of fundamental interest; in addition, collision processes such as ionization and charge transfer occur in many applied areas, e.g., accelerator design and beam transport, fusion, and production of slow highly charged recoil ions for subsequent collision studies. We discuss here our recent work on ionization, charge transfer, and recoil-ion production, for fast highly charged ions in H₂ and rare-gas targets. Projectile energies are in the range 100 keV amu⁻¹ to 8.4 MeV amu⁻¹ for charge states 3+ to 59+. We also present classical-trajectory Monte Carlo (CTMC) calculations for ionization and recoil-ion production, and compare the results with experiment.

2. Ionization

We have studied ionization of gas targets by fast highly stripped projectiles using three methods:

(1) measurement of net ionization or total charge produced in a gas target by passage of a fast projectile. We designate the cross-section for this process σ_+ . The condenser-plate method was used.

(2) measurement of recoil-ion charge-state fractions created by passage of a fast projectile through a gas jet. We used a time-of-flight coincidence technique. The cross-section for producing a recoil ion in charge state j is σ_j . We obtained cross-sections σ_j by normalizing measured charge-state fractions to measured net-ionization cross-sections σ_+ :

$$\sigma_+ = \sum j \sigma_j. \quad (1)$$

(3) calculations using the CTMC method to obtain cross-sections for ionization of hydrogen with extension to multi-electron targets by use of the independent-electron model.

* This work was supported by the Director, Office of Energy Research, Office of Fusion Energy, Applied Plasma Physics Division, of the U.S. Department of Energy under Contract No. DE-AC02-82ER53128 and DE-AC03-76SF00098.

† On leave in 1981 at Universität Giessen.

2.1. Net ionization [1]

A beam of fast ions from the SuperHILAC accelerator located at the Lawrence Berkeley Laboratory was stripped in a foil; a beam in a single charge state was selected by a magnetic analyser. Slow ions or electrons produced by passage of this beam through a gas target (Fig. 1) were swept from a well-defined length of the target by a weak transverse electric field. The primary beam was measured with a Faraday cup. The net-ionization cross-section is determined from the ratio of collected ion current to primary beam particle current, divided by target thickness. We performed such measurements in H₂ and in rare gases for a wide variety of projectiles (carbon, iron, niobium, and lead ions) in charge states as low as 3+ to as high as 59+, and for energies in the range 100 keV amu⁻¹ to 4.7 MeV amu⁻¹. Typical results are shown in Fig. 2.

2.2. Recoil-ion production [2]

A time-of-flight (TOF) coincidence technique (Fig. 3) was used to measure recoil-ion charge-state fractions. A 1.4 MeV amu⁻¹ U⁴⁴⁺ beam from the UNILAC accelerator at GSI in Darmstadt intersected a beam of rare-gas atoms emerging from a tube. Slow recoil ions produced in the collision were extracted by a transverse electric field and accelerated onto a channeltron. The channeltron pulse and a pulse created by the fast beam were fed to a time-to-amplitude converter (TAC) to measure the flight time of the recoil ions, and thus their charge-state distribution was determined. A TOF spectrum for 1.4 MeV amu⁻¹ U⁴⁴⁺ in Ne is shown in Fig. 4. Similar results have been obtained by Cocke using lower-charge-state projectiles [3]. Recoil-ion-production cross-sections were determined by normalization of the recoil-ion charge-state fractions to net-ionization cross-sections.

2.3. Classical-trajectory Monte Carlo calculations [1, 4]

The theoretical calculations use the 3-body classical-trajectory Monte Carlo (CTMC) method to determine transition probabilities within a one-electron formalism. By using an ionization energy and an effective charge that characterize an electron shell of a multielectron target, multiple-electron ionization cross-sections may be calculated using the independent-electron model [5, 6]. The independent-electron model requires that the collision be sudden, with the collision period sufficiently brief that the electrons cannot rearrange themselves during the collision. The calculation is only expected to be qualitative for production of highly charged recoil ions, since many approximations are necessary in extending a one-electron calculation to

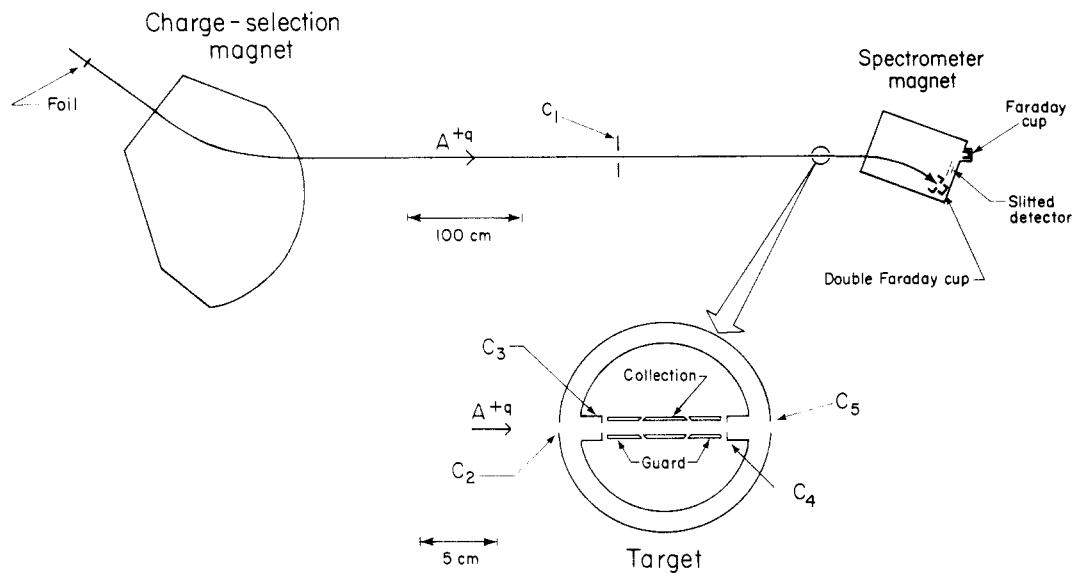


Fig. 1. Schematic diagram of LBL apparatus. Net-ionization cross-sections were measured by collecting the slow-ion and slow-electron current in the gas target.

a many-electron target. The model ignores correlation effects between the electrons in a given shell; also not accounted for are autoionization processes after the collision.

2.4. Results: net ionization

Experimental and theoretical net-ionization cross-sections σ_+ for 1.1 MeV amu⁻¹ projectiles in various charge states are shown in Fig. 2. The good agreement between experiment and the CTMC calculation is evident.

We found [1] that the calculated net-ionization cross-sections σ_+ for a given rare-gas target reduce to a common curve when

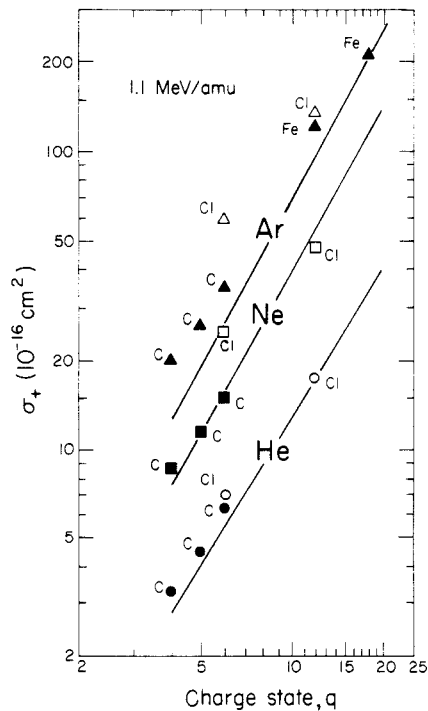


Fig. 2. Net-ionization cross-sections for 1.1 MeV amu⁻¹ projectiles in charge state q in He (\bullet , \circ), Ne (\blacksquare , \square), and Ar (\blacktriangle , \triangle) targets. The closed symbols are experimental results [1] for 1.15 MeV amu⁻¹ C and Fe projectiles, the open symbols are experimental results for Cl projectiles (adjusted to 1.1 MeV amu⁻¹) by Cocke [3], and the lines are the CTMC calculations for 1.1 MeV amu⁻¹.

plotted in the reduced coordinates σ_+/q and E/q , where E is projectile energy per nucleon and q is projectile charge state. The experimental results also reduce to a single curve in these reduced coordinates. Results are shown in Fig. 5. The CTMC curves are proportional to q^2/E at the highest values of E/q , while the experimental results tend towards $q^{3/2}/E^{1/2}$, and thus lie increasingly above the CTMC curve for increasing values of E/q . Results agree generally, however, to within a factor of 2.

2.5. Results: recoil-ion production

The measured recoil-ion-production cross-sections σ_j for 1.4 MeV amu⁻¹ U⁴⁴⁺ in rare-gas targets are compared with the calculated values in Fig. 6. Net-ionization cross-sections σ_+ are found to be very large and to exceed 10⁻¹³ cm² for the heavy rare-gas targets. It is clear from the comparison between theory and experiment that σ_+ is reasonably portrayed by the calculations, but that the recoil-ion-production cross-sections σ_j predicted by theory are only qualitative.

The deficiencies in the theoretical description probably arise from two approximations that are necessary to perform the calculations. The independent-electron model requires the use

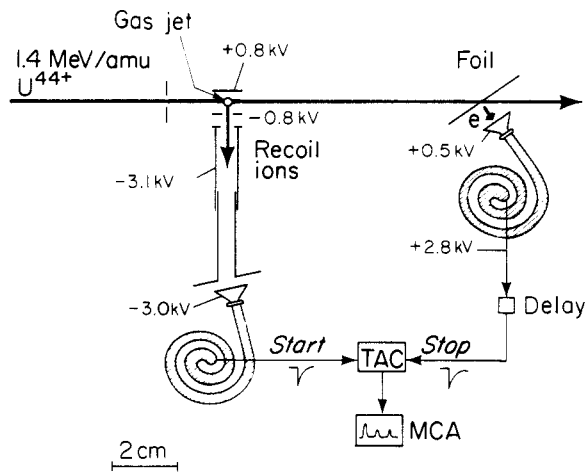


Fig. 3. Schematic diagram of the TOF-coincidence apparatus used to measure recoil-ion charge-state spectra at GSI.

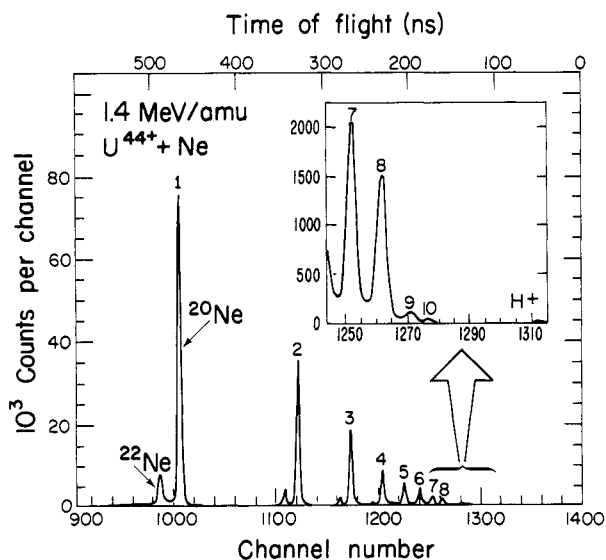


Fig. 4. Recoil-ion charge-state spectrum for $1.4 \text{ MeV amu}^{-1} \text{ U}^{44+}$ projectiles in a thin Ne target. Neon recoil charge states 1+ to 10+ are labeled, as is a background H^+ peak. The small peaks to the left of the larger peaks are due to the ^{22}Ne isotope.

of an average binding energy for all electrons within a given shell. If the collision is not sufficiently sudden and the electrons are removed sequentially this approximation fails, with the result that the last few electrons removed from a shell have a binding energy much larger than the average value of the model. Thus, the calculations will generally overestimate the cross-sections for production of the higher charge states.

The theoretical underestimation of the cross-sections for low-charge-state recoil-ion production reflects the classical description of the radial electron distribution in the target atom. Tunnelling is not allowed classically, hence the electron distribution is not accurately portrayed at large electron-nucleus separations. The low-charge-state recoil ions are generated by

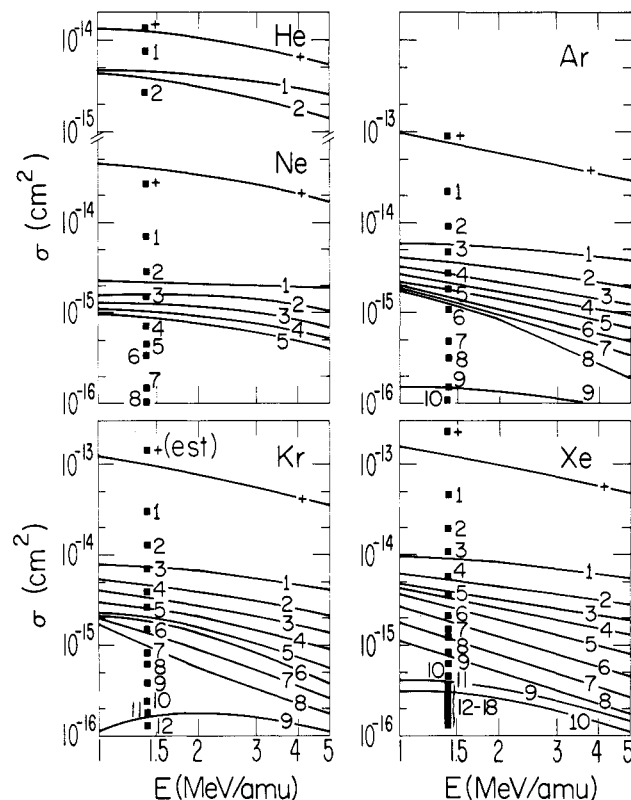


Fig. 6. Cross-sections σ_j for production of j -times-ionized recoil ions in He, Ne, Ar, Kr, and Xe targets. The lines are the CTMC calculations for $1\text{--}5 \text{ MeV amu}^{-1}$ projectiles in charge state $44+$, the points are experimental results for $1.4 \text{ MeV amu}^{-1} \text{ U}^{44+}$. The experimental σ_j are normalized to experimental σ_+ values (for Kr the σ_+ value shown was estimated).

large-impact-parameter (soft) collisions that are sensitive to this region of the target's electron distribution. Comparison of theory with experimental data indicates that the collisions are of longer range than we calculate.

Figure 7 shows recoil-ion fractions F_j ($F_j = \sigma_j / \sum \sigma_j$). Theor-

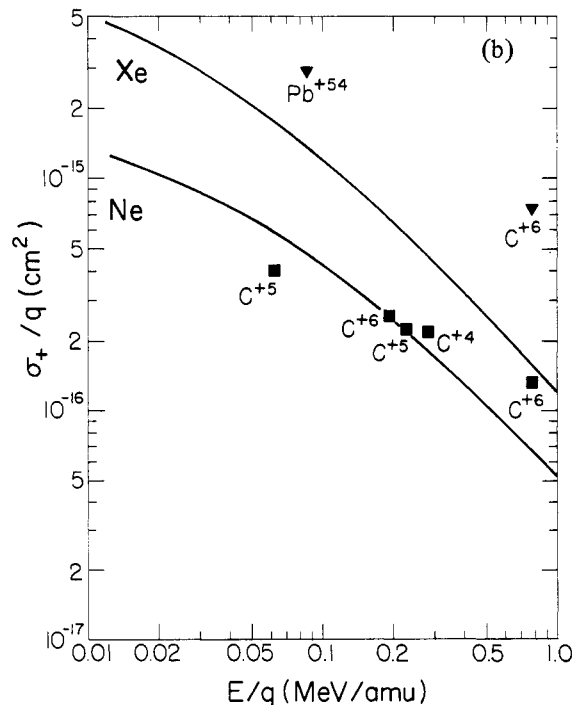
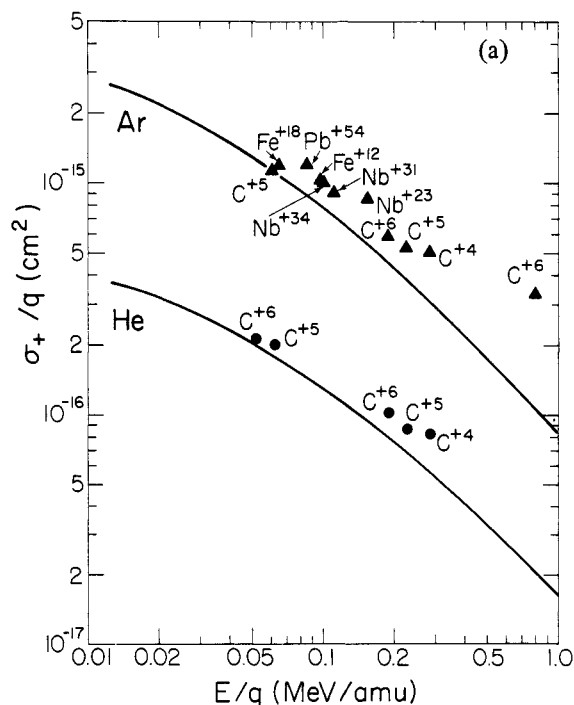


Fig. 5. Reduced plot of net-ionization cross-sections for a highly stripped ion in charge-state q in He (●) and Ar (▲) targets (a) and in

Ne (■) and Xe (▼) targets (b). The closed symbols are experimental results, and the curves are the CTMC calculations.

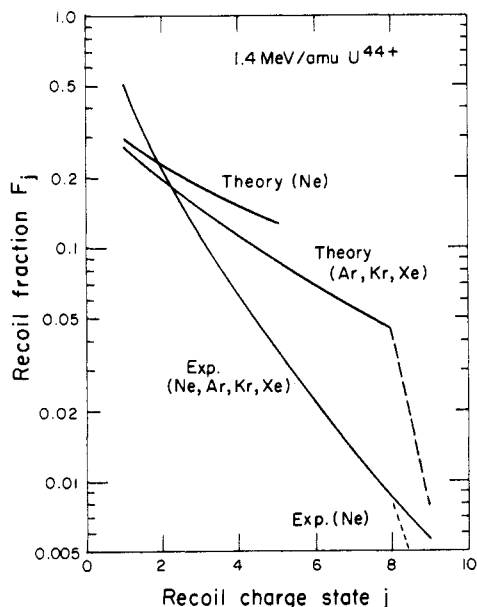


Fig. 7. Recoil-ion charge-state fractions F_j for 1.4 MeV amu^{-1} U^{44+} in Ne, Ar, Kr, and Xe. The theoretical lines are the CTMC calculations. The dashed lines indicates discontinuity due to shell effects.

etical F_j for Ar, Kr, and Xe were found to lie on a single curve; experimental F_j were also found to lie on a common curve (except for F_9 and F_{10} in Ne). The calculations show a pronounced effect due to the shell structure of the target atom, while (except for Ne) the experimental data do not, which indicates that Auger processes must contribute significantly to the production of highly charged recoil ions; this mechanism is not included in the calculations.

Collisions in which rare-gas targets are ionized by fast highly stripped projectiles generally take place at long range. The ionization transition probabilities as a function of impact parameter are calculated using the CTMC method previously discussed. We graphically display in Fig. 8 the long-range nature of these collisions by presenting the sum of the calculated ionization transition probabilities as a function of impact parameter for a 2 MeV amu^{-1} fully stripped ion in charge state 44+ in rare-gas targets. The expectation value for the radius of the outer shell of each rare-gas atom is indicated by an arrow. The collision region is seen to extend to approximately ten times the radii of the outer electron shells.

2.6. Recoil-ion energy

The classical-trajectory method was also used to estimate the energy of the recoil ions. This calculation can also be done analytically if one assumes the projectile velocity is much greater than the final velocity of the recoil ion. An illustrative example is the production of Ar^{10+} from U^{44+} impact at 1 MeV amu^{-1} . The calculated probabilities for the above ionization transition maximize at an impact parameter $b = 2a_0$ and extend to $b = 1a_0$ and $3a_0$. The corresponding recoil energies extend from 0.2 eV to 5 eV with a maximum at 1 eV; high recoil energies correspond to small impact parameters.

We have parameterized the theoretical CTMC results and find the recoil energy E_t (in eV) is given by

$$E_t = \frac{c_r q_p^2 q_t^2}{m_t E_p b^2} \quad (2)$$

where q_p and q_t are the charge states of the projectile and recoil ions, respectively, m_t is the mass of the target in atomic mass

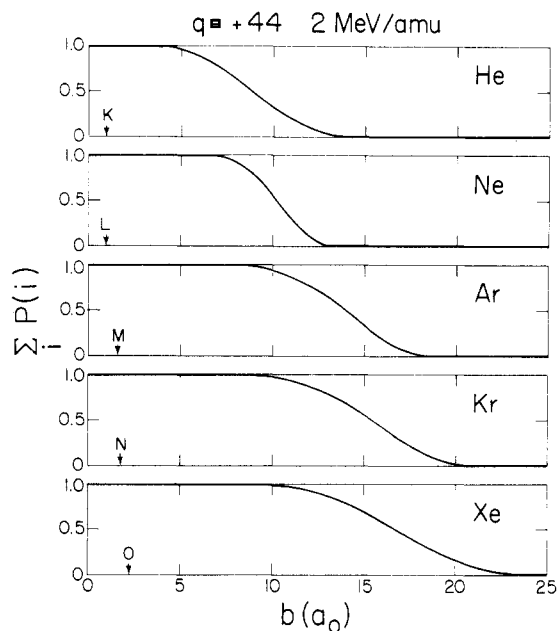


Fig. 8. Total calculated ionization probabilities for a 2 MeV amu^{-1} projectile in charge state 44+ in rare-gas targets. The arrows indicate the expectation value for the radius of the outer shell of the target atom.

units, E_p is the energy of the projectile in MeV amu^{-1} and b is the impact parameter in units of a_0 . The coefficient c_r equals 4×10^{-4} if one assumes the projectile-target nucleus interaction is zero until the distance of closest approach, where the electrons are ejected; the projectile-target nucleus interaction is Coulombic for the rest of the trajectory. Our calculations indicate that there is incomplete screening of the target nucleus on the inward portion of the trajectory and that c_r can be several times larger than the 4×10^{-4} Rutherford value. The most probable recoil-ion energy is found to correspond to c_r approximately equal to 6×10^{-4} . The recoil-ion energy decreases rapidly with increasing impact parameter and is generally less than 10 eV for the systems studied here.

Equation 2 for the recoil-ion energy, obtained by parameterizing the CTMC calculations, has the same functional dependence as obtained for Rutherford (Coulomb) scattering. The coefficient in eq. (2) is slightly greater than one half the coefficient for Rutherford scattering. We note that eq. (2) can be used to determine the impact-parameter dependence of the collision process by measurement of the recoil-ion energy distribution.

2.7. Ionization of rare-gases: summary

Net-ionization cross-sections σ_+ are well predicted by the CTMC calculations, while recoil-ion-production cross-sections σ_j are only qualitatively predicted. Net-ionization cross-sections are found to scale in reduced coordinates σ_+/q and E/q for a very wide range of projectile species, charge states, and energies. Ionization takes place at long range, extending to 10 times the radius of the outer electron shell. Recoil-ion-production cross-sections are large, even for highly stripped recoil ions; for example, 1.4 MeV amu^{-1} U^{44+} produces Ne^{8+} , Ar^{10+} , Kr^{12+} , and Xe^{18+} with cross-sections greater than $1 \times 10^{-16} \text{ cm}^2$. Recoil-ion energies are low, typically less than 10 eV; recoil ions are thus useful for subsequent low-energy collision studies [7].

2.8. Ionization of hydrogen

We have previously shown [8] that CTMC calculations for

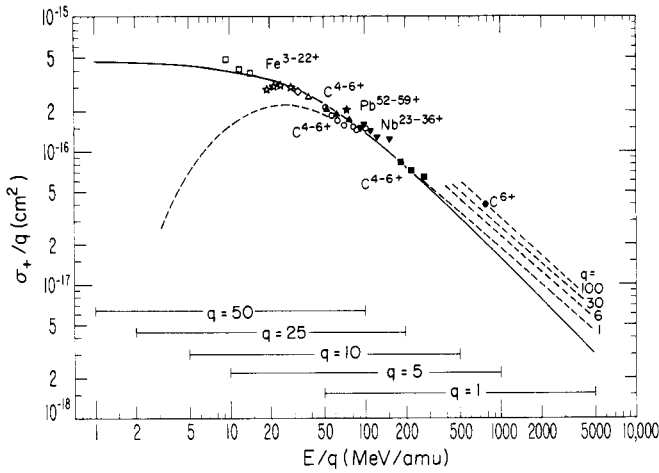


Fig. 9. Reduced plot of electron-removal cross-section for a fast highly charged ion in charge state q in atomic hydrogen. Solid line is CTMC calculation, points are experimental cross-sections in H_2 divided by 2. The dashed lines are the Born approximation for ionization, to which the data should tend for large values of E/q .

electron removal from an atomic hydrogen target reduce to a single curve in the scaled coordinates σ_+/q and E/q . Experimental electron-removal cross-sections in H_2 divided by 2 agree well with the CTMC calculations, except for large values of E/q , where the experimental results were found [9] to be larger than the Born approximation for H as well as the CTMC result. This arises [10, 11] because the limiting Born-approximation result for σ_+ is proportional to $q^2 (\ln E)/E$, which does not reduce to a single curve in the reduced coordinates σ_+/q and E/q . This is easily shown by changing variables to $\sigma_+^r = \sigma_+/q$ and $E^r = E/q$. Then $q (\ln E)/E$ becomes $\ln(qE^r)/E^r$, and we obtain a closely spaced family of curves (Fig. 9) rather than a single curve for σ_+^r for large values of E^r . Shah and Gilbody [12] have recently measured ionization in H_2 and H and have shown that the cross-section ratio is approximately 2 for fast projectiles. They have also confirmed [13] that σ_+^r lies above the CTMC and Born-approximation calculations for H for large values of E^r ; σ_+ for sufficiently fast fully stripped projectiles is found to agree with the Born approximation.

3. Electron capture in H_2 and in rare gases

We previously obtained [14] an empirical scaling rule for electron-capture cross-sections $\sigma_{q,q-1}$ for fast highly charged iron ions Fe^{q+} in H_2 : $\sigma_{q,q-1}$ scales as $q^{3.15} E^{-4.48}$ for projectile energies greater than 275 keV amu^{-1} . We have extended [15] this empirical scaling to targets with atomic number z : electron-capture cross-sections for fast highly charged projectiles reduce to a common curve when plotted in the reduced coordinates $\sigma_{q,q-1} z^{1.5}/q^{0.95}$ and $E/(q^{0.5} z^{1.1})$, where q is projectile charge state, E is projectile energy in keV per amu, and z is target atomic number. This preliminary result is shown in Fig. 10. Using the reduced parameters \tilde{E} and $\tilde{\sigma}$

$$\begin{aligned} \tilde{E} &= E/(q^{0.5} z^{1.1}) \\ \tilde{\sigma} &= \sigma z^{1.5}/q^{0.95} \end{aligned} \quad (3)$$

we can write the equation for the empirically determined curve shown in Fig. 10 as

$$\begin{aligned} \tilde{\sigma} &= 8.8 \times 10^{-16} \times 5 \times 10^6 [1 - \exp(-\tilde{E}^{1.7}/70)] \\ &\times [1 - \exp(-\tilde{E}^{2.8} \times 70/(5 \times 10^6))]/\tilde{E}^{4.5}. \end{aligned} \quad (4)$$

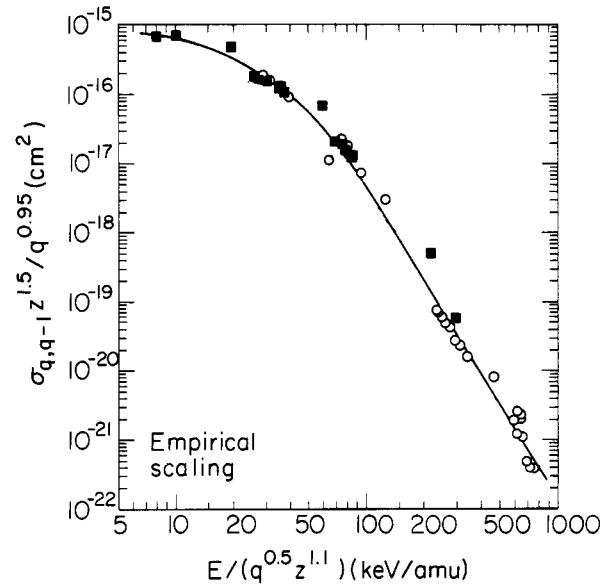


Fig. 10. Reduced plot of single-electron-capture cross-section for a fast highly charged ion in charge state q in a rare-gas (closed symbol) or H_2 (open symbol) target with atomic number z . Cross-sections in H_2 are divided by 2 and treated as $z = 1$. The line is an empirical fit to the data.

We also find in this empirical fit that H_2 cross-sections can be treated by dividing the cross-section by 2 and then using $z = 1$. The empirical scaling that we obtain is similar to the scaling for high reduced energy obtained by Knudsen et al. [16] based on Bohr-Lindhard cross-sections and the Lenz-Jensen atomic model.

At high reduced energies, eq. 4 asymptotically approaches the following:

$$\sigma = 4.4 \times 10^{-9} q^{3.2} z^{3.45}/E^{4.5}. \quad (5)$$

This q and E dependence are in approximate agreement with our previous results for an H_2 target. The target z dependence is a new result, which can be used to predict cross-sections in a wide variety of targets.

The treatment of H_2 as a $z = 1$ target with the cross-section divided by 2 that we determined empirically is not what would be expected on the basis of recent work of Knudsen et al. [17], who found, for electron capture by fast highly charged projectiles, that the cross-section ratio for H_2 and H targets is about 3.8. The apparent factor of 2 we find empirically does not necessarily imply that this is, in fact, the ratio of the electron-capture cross-sections in H_2 and H, since it could be an artifact of the fitting process. Investigations of this factor for large values of reduced energy would be of interest to clarify this point.

Acknowledgements

This work was supported in part by the U.S. Department of Energy under contracts DE-AC02-82ER53128 and DE-AC03-76SF00098. One of us (A.S.) would like to thank Professor Erhard Salzborn for his hospitality during my stay in Giessen, and to acknowledge support from NATO (Research Grant 172.80) and from the Alexander von Humboldt Stiftung.

References

- Schlachter, A. S., Berkner, K. H., Graham, W. G., Pyle, R. V., Schneider, P. J., Stalder, K. R., Stearns, J. W., Tanis, J. A. and

- Olson, R. E., Phys. Rev. **A23**, 2331 (1981).
2. Schlachter, A. S., Groh, W., Müller, A., Beyer, H. F., Mann, R. and Olson, R. E., Phys. Rev. **A26**, 1373 (1982).
3. Cocke, C. L., Phys. Rev. **A20**, 749 (1979).
4. Olson, R. E., J. Phys. **B12**, 1843 (1979).
5. Hansteen, J. M. and Mosebekk, O. P., Phys. Rev. Lett. **29**, 1361 (1972).
6. McGuire, J. H. and Weaver, L., Phys. Rev. **A16**, 41 (1977).
7. Beyer, H. F., Schartner, K. H. and Folkmann, F., J. Phys. **B13**, 2459 (1980); Mann, R., Beyer, H. F. and Folkmann, F., J. Phys. **B14**, 1161 (1981); Mann, R., Beyer, H. F. and Folkmann, F., Phys. Rev. Lett. **46**, 646 (1981); Vane, C. R., Prior, M. H. and Marrus, R., Phys. Rev. Lett. **46**, 107 (1981); Cocke, C. L., Du Bois, R., Gray, T. J., Justiniano, E. and Can, C., Phys. Rev. Lett. **46**, 1671 (1981); Justiniano, E., Cocke, C. L., Gray, T. J., Dubois, R. and Can, C., Phys. Rev. **A24**, 2953 (1981).
8. Olson, R. E., Berkner, K. H., Graham, W. G., Pyle, R. V., Schlachter, A. S. and Stearns, J. W., Phys. Rev. Lett. **41**, 163 (1978).
9. Schlachter, A. S., Berkner, K. H., Graham, W. G., Pyle, R. V., Stearns, J. W. and Tanis, J. A., Phys. Rev. **A24**, 1110 (1981).
10. Gillespie, G. H., Phys. Rev. **A24**, 608 (1981).
11. Shah, M. B. and Gilbody, H. B., Private communication.
12. Shah, M. B. and Gilbody, H. B., Submitted to J. Phys. B.
13. Shah, M. B. and Gilbody, H. B., J. Phys. **B15**, 413 (1982).
14. Berkner, K. H., Graham, W. G., Pyle, R. V., Schlachter, A. S. and Stearns, J. W., Phys. Rev. **A23**, 2891 (1981).
15. Stearns, J. W., Graham, W. G., Berkner, K. H., Pyle, R. V., Schlachter, A. S. and Tanis, J. A., To be submitted to Phys. Rev. A.
16. Knudsen, H., Haugen, H. K. and Hvelplund, P., Phys. Rev. **A23**, 597 (1981).
17. Knudsen, H., Haugen, H. K. and Hvelplund, P., Phys. Rev. **A24**, 2287 (1981).